Mon. Not. R. astr. Soc. (1990) **243**, 126–132

A millimetre/submillimetre common user photometer for the James Clerk Maxwell Telescope

W. D. Duncan,[1] E. I. Robson,[2] P. A. R. Ade,[3] M. J. Griffin[3] and G. Sandell[1]

[1] *Joint Astronomy Centre, 665 Komohana St., Hilo, HI 96720, USA*
[2] *School of Physics & Astronomy, Lancashire Polytechnic, Preston PR1 2TQ*
[3] *Department of Physics, Queen Mary College, Mile End Rd, London E1 4NS*

Accepted 1989 August 30. Received 1989 August 25; in original form 1989 March 22

SUMMARY

We describe a multi-wavelength common user millimetre/submillimetre receiver which is now in operation on the James Clerk Maxwell Telescope (JCMT)* on Mauna Kea, Hawaii. It is a single channel photometer employing a composite germanium bolometric detector cooled by helium-3 to 0.35 K. The receiver has a set of bandpass filters allowing observations to be made in all of the atmospheric transmission windows between 350 μm and 2 mm.

1 INTRODUCTION

Submillimetre astronomy is only now beginning to emerge from almost two decades of slow progress by a few persistent groups around the world. This region of the spectrum, extending from wavelengths of a few millimetres to 100 μm, is beset by problems for ground-based observers. The atmospheric transmission is poor over most of this region. The absorption is due primarily to rotational transitions of water vapour and oxygen. Observations at wavelengths shorter than 350 μm can only be made from airborne or satellite platforms. Between 350 μm and 2 mm, there are a number of semi-transparent 'windows' through which it is possible to observe from a high-altitude, dry site. Fig. 1 shows the near-millimetre transmission spectrum at the summit of Mauna Kea for various amounts of precipitable water vapour (ω) for which a value of 1–2 mm is typical but, on very dry occasions, may fall to around 0.5 mm. It is clear that from this site it is feasible to observe through the windows at around 350, 450, 600, 750 and 850 μm, and at wavelengths longer than about 1 mm. Even at this high altitude (4200 m), observations at 350 and 450 μm windows are difficult due to atmospheric absorption.

Besides attenuating the signal from the source, the atmosphere has a number of other unwelcome effects. Thermal emission from the sky (and the telescope) degrades the available sensitivity by contributing photon noise and by thermally loading the cooled detector. Spatial and temporal variations in sky emission on scales comparable to the chop throw or frequency result in imperfect sky background cancellation or 'sky noise'. This often proves to be the main limit to sensitivity, especially in the 350 and 450 μm windows. Additionally, the combination of a turbulent atmosphere and a large telescope produces sufficient phase changes across the wavefront to produce random changes in the telescope pointing of up 60 arcsec in extreme conditions. This 'refraction' noise typically persists for up to 2 h after sunset in moderate to poor water vapour conditions (Kemp 1980; Altenhoff *et al.* 1987).

Although difficult, obervations in the submillimetre region are of great importance for a wide range of astrophysical studies (e.g., Wolstencroft & Burton 1988; Emerson 1988). In the continuum, the areas of study range from: planetary surfaces and atmospheres, thermal emission from dust in star formation regions, evolved stars and galaxies; synchrotron emission from active galactic nuclei and supernova remnants; the cosmic background radiation. Observations of the submillimetre continuum emission from dust are particularly important, and provide an essential complement to spectral line data in probing molecular cloud structure, cloud masses and gas densities. The interpretation of the predominately optically thin dust continuum emission, whilst far from trivial, is simpler and far less model dependent than the analysis of molecular line observations. The latter are prone to optical depth and excitation effects and considerable uncertainties in chemical abundances.

The importance of the millimetre/submillimetre region has been increasingly recognized in recent years, and several large-diameter telescopes have been purpose-built to operate at these wavelengths.

In this paper, we describe a common user photometer, UKT14, designed to operate both on the 3.8-m UKIRT infrared telescope and the 15-m JCMT millimetre/submillimetre telescope. This instrument was built by the Royal Observatory Edinburgh in collaboration with Queen Mary College and the University of Oregon. Its basic design is modelled on the QMC/Oregon photometer (Ade *et al.* 1984; Griffin 1985) which was used on UKIRT for a number of years. UKT14 was first commissioned on UKIRT in 1986 January, and was successfully operated on that telescope

*The JCMT is operated by the Royal Observatory Edinburgh on behalf of the SERC, The Netherlands ZWO and the Canadian NRC.

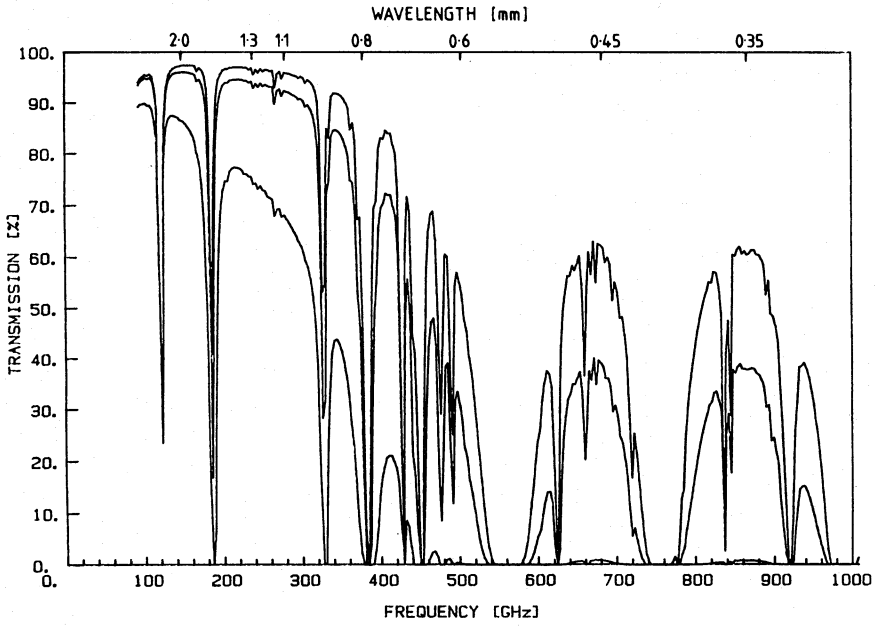

Figure 1. Atmospheric transmission from Mauna Kea for values of precipitable water vapour of 0.5, 1 and 5 mm.

until 1988 February. It has now been moved permanently to the JCMT and has already been used to make major advances in observational submillimetre astronomy (Edelson *et al.* 1988, and papers in Watt & Webster 1989).

2 OPTICAL DESIGN

There are four main elements in the design of a millimetre/submillimetre photometer: the detector, a cooled semiconductor bolometer; filters which define the spectral pass-bands; the optical system which concentrates the radiation collected by the telescope on to the detector; and the cryostat for cooling the detector and as much of the optics as is practical.

Telescopes designed for infrared and near-millimetre wavelengths have large Cassegrain focal ratios (>10), so as to make the secondary mirror small enough that it can be nutated rapidly to perform sky chopping. This leads to difficulties in the optical and cryogenic design of near-millimetre systems owing to the large diffraction spot size. UKT14 was designed to operate, in the first instance, at the $f/36$ Cassegrain focus of UKIRT. The diameter of the Airy disc (given by $2.44\lambda f$) at 1 mm wavelength is about 90 mm for this focal ratio. A large focal plane aperture was therefore needed (Duncan 1983). To accommodate UKT14 on the JCMT without internal modification, the receiver is located on the Nasmyth platform and is fed through the hollow elevation bearing via a hyperbolic tertiary. The tertiary converts the Cassegrain $f/12$ beam to $f/36$ at the Nasmyth focus. The remainder of this paper will describe the operation and performance of UKT14 on the JCMT.

The essential features of the photometer are shown in Fig. 2. A 70-mm diameter polyethylene field lens at the telescope focal plane converts the $f/36$ beam to $f/3$ and directs the radiation through a 5-mm aperture and bandpass filter. The filter is directly in front of the entrance aperture of a Winston light concentrator (Harper *et al.* 1976). A continuously adjustable iris placed in front of the lens is used to set the focal plane aperture. The maximum usable lens diameter is limited to 65 mm in order to avoid extraneous diffraction effects from the cryostat window. This is limited in size due to heat input and consequent loss in cryogen hold-time. In order to reduce the background power on the bolometer as much as possible, the lens/iris combination is cooled by direct thermal contact with the 77 K radiation shield.

The light cone and the detector are mounted on the helium-3 work surface at a temperature of 0.35 K. The bandpass filters and associated apertures are contained in a 10-position filter wheel mounted on the helium-4 work surface. The filter wheel is rotated under computer control by a stepper motor outside the cryostat. The thermal input to the cryostat is minimized by a filter on the 77 K radiation shield which blocks out wavelengths shorter than 100 μm. A low-pass mesh filter (edge at 300 μm), located in front of the filter wheel and at a temperature of 4 K, excludes far-infrared radiation at wavelengths shorter than about 300 μm. The

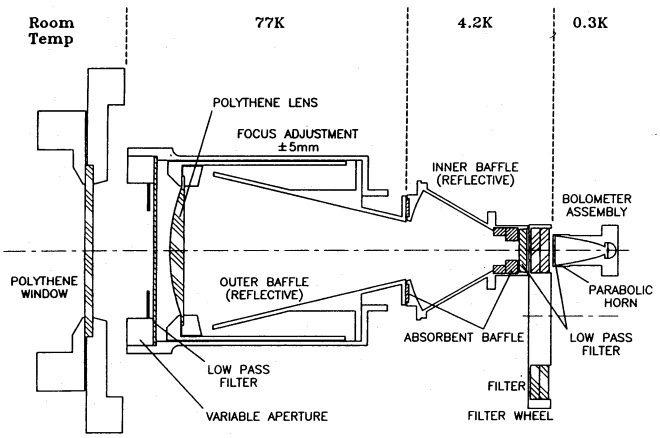

Figure 2. Optical arrangement of UKT14.

bolometer is shielded from the possibility of seeing scattered optical and infrared radiation by a further filter located at the concentrator entrance aperture. In order to eliminate small harmonic leaks which fall within the transmission range of 300-μm filter, some of the bandpass filters are constructed with additional blocking filters.

The maximum aperture of 65 mm limits the geometric field of view of the photometer to about 22 arcsec and taking diffraction effects into consideration provides beamwidths ranging from 19 arcsec at 1.1 mm to 18 arcsec at 450 μm, with a dip to 16 arcsec at 800 μm. If high spatial resolution is required then the iris diameter may be set under computer control to one of the preset series of apertures corresponding to the diffraction limit for the main filters. For wavelengths longward of 1.1 mm, the optics efficiency decreases rapidly with increasing wavelength since the diffraction spot gets larger relative to the size of the optics. At 1.1 mm, the efficiency is around 70 per cent, decreasing to about 10 per cent at 2 mm (Duncan 1983).

Each of the basic elements of the photometer system will now be described in more detail.

3 FILTERS

Accurate knowledge of the effective wavelength of observation is crucial to the correct interpretation of continuum data. The effective wavelength depends on the overall transmission profile of the photometer, on the atmospheric transmission and airmass of the observation, and on the spectral index of the source. It also depends on the surface accuracy of the antenna and the spatial extent of the source. As with most photometers, bandpass filters are used to restrict the transmission within the overall wavelength response of the photometer to a series of well defined and much narrower spectral windows.

The most obvious advantages in using a narrow filter pass-band are that it minimizes the sensitivity of the effective wavelength to the atmospheric conditions, the source spectral index and the antenna surface, allowing more accurate definition of the source spectrum. However, in many applications this might be offset by the fact that a narrow pass-band reduces system sensitivity because of the reduction in the total power collected from the astronomical source.

Simple considerations suggest that in a photon noise-dominated system the sensitivity will be nearly proportional to the square root of the bandwidth. However, for ground-based mm–submm observations, this is more than offset by two further advantages of having a narrow pass-band: (i) it reduces the thermal background power on the detector, thereby yielding an increase in sensitivity (Griffin & Holland 1988); (ii) it is found in practice that it also reduces the severity of excess sky noise.

The bandpass filters in UKT14 are tailored to allow observations in the main atmospheric windows between 350 μm and 2 mm. The principal filters used are listed in Table 1, together with their centre frequencies and pass-bands. Transmission profiles for most of the filters are shown in Fig. 3. The effective wavelength is a function of line-of-sight water vapour, source spectral index and dish accuracy. It is necessary to model these effects to obtain accurate fluxes. Table 2 lists the effective frequencies for various amounts of precipitable water vapour, ω(mm), and source spectral index, n, for a dish surface accuracy of 35 μm. Note that with the exception of the WBMM filter, the effective frequencies vary by only a few per cent over a wide range of observing conditions.

Table 1. UKT14 Filters.

FILTER	CENTRE FREQUENCY (GHz)	PASSBAND (GHz)
2.0 mm	149	40
1.3 mm	233	64
1.1 mm	266	74
WBMM	290	220
850μm	354	30
800μm	384	101
600μm	480	112
450μm	682	84
350μm	864	113

Table 2. Variation of filter effective frequencies with source spectral index (n) and atmospheric water vapour (ω).

FILTER	EFFECTIVE FREQUENCY FOR w = 1 mm (GHz)			EFFECTIVE FREQUENCY FOR n = 2 (GHz)			
	$n = 0$	$n = 2$	$n = 4$	$w = 0.5$	$w = 1$	$w = 2$	$w = 4$
2.0 mm	149.1	155.6	177.6	156.7	155.6	154.3	153.0
1.3 mm	233.2	237.9	243.8	238.3	237.9	237.5	237.1
1.1 mm	265.9	271.6	278.1	272.3	271.6	270.6	269.3
WBMM	291.7	316.9	342.6	323.1	316.9	308.1	296.0
850μm	351.0	353.0	354.3	353.3	353.0	352.6	351.9
800μm	372.9	379.5	385.9	381.7	379.5	375.9	370.1
600μm	457.8	463.0	467.8	469.8	463.0	451.5	434.3
450μm	673.7	675.8	677.8	677.1	675.9	674.4	672.9
350μm	850.8	854.9	858.3	856.3	854.9	854.0	854.0

4 BOLOMETER

The detector is a composite Ge:In:Sb bolometer (El-Ataway *et al.* 1980; Griffin 1985) mounted in a hemispherical integrating cavity. Fig. 4 shows a set of load curves for the bolometer when viewing the sky at the zenith (under good conditions) through the various filters, and illustrates the increase in background power loading with decreasing wavelength. The background tends to warm up the detector, which manifests itself as a flattening of the load curve. Although this is accompanied by a degradation in the inherent sensitivity of the detector, the performance at the shorter wavelengths is limited by the excess sky noise rather than the detector itself.

The measured optical NEP of the detector in the laboratory in the 1.1 mm waveband is 10^{-15} W Hz$^{-1/2}$. Allowing for all losses in the filters and optics, this corresponds to a system NEP (for comparison purposes this is referred to the input of the system – the cryostat window) of 5×10^{-15} W Hz$^{-1/2}$. The responsivity of the detector decreases with increasing modulation frequency with a 3dB point at 70 Hz. This is well above the usual JCMT chopping frequency of about 8 Hz.

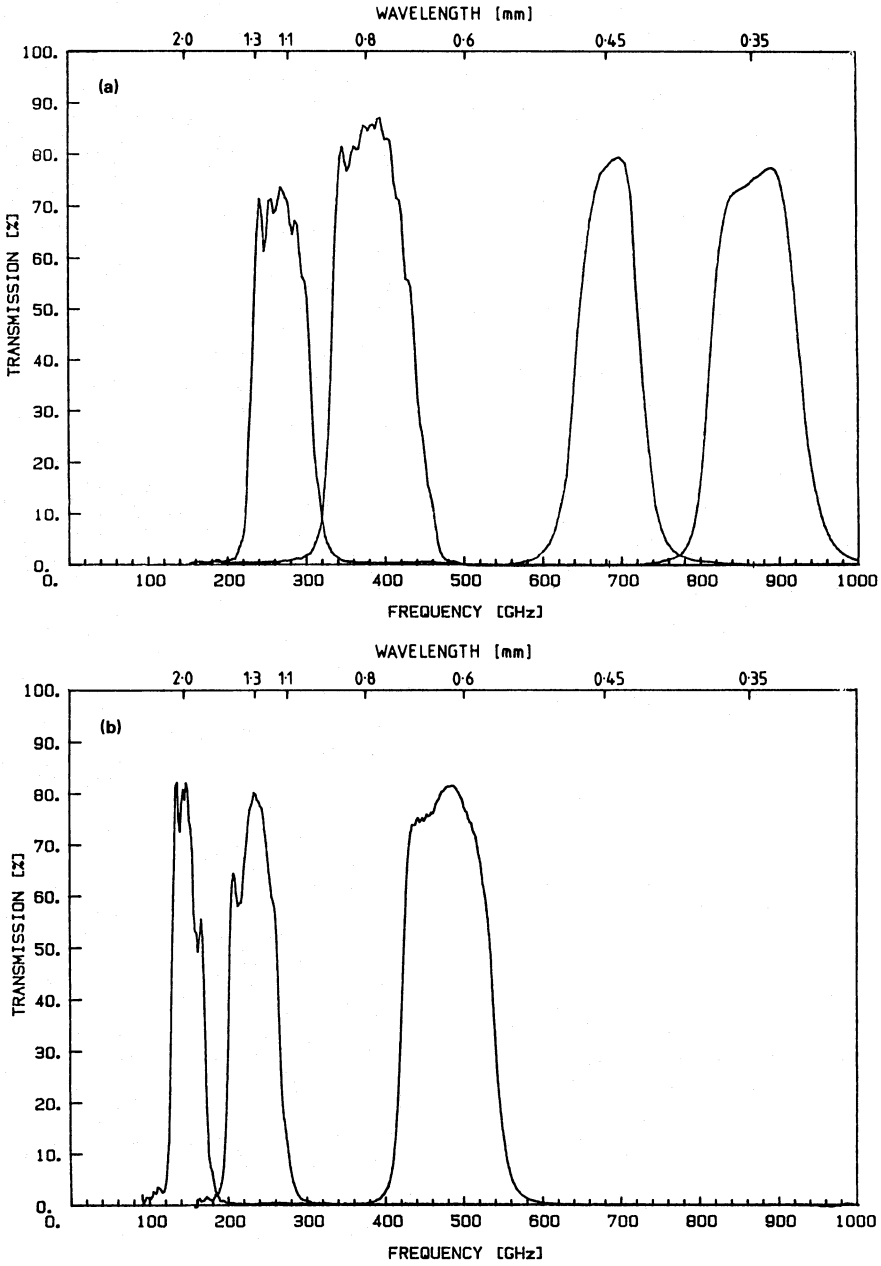

Figure 3. (a) Filter profiles for the 1.1, 0.8, 0.45 and 0.35 mm pass-bands, (b) filter profiles for the 2.0, 1.3 and 0.6 mm pass-bands.

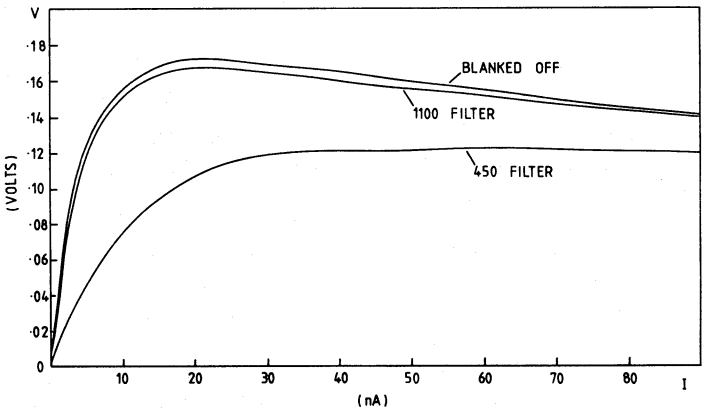

Figure 4. V–I curves for the UKT14 bolometer.

The bolometer resistance at the operating point is around 2 MΩ. This is small enough to allow the use of a room temperature pre-amplifier. The UKT14 pre-amplifier (Cochise Instruments Inc.), with a gain of 10^3, is bolted to the outside of the dewar. It has an input-short noise of 4 nV Hz$^{-1/2}$, and contributes a negligible amount to the overall noise.

5 CRYOSTAT

The helium-3 system, manufactured by Cochise Instruments Inc., is contained in a custom-modified Janis Helium-4 dewar of 6 litre capacity. When the system is warm, the 10 STP litre charge of helium-3 gas is stored in an external tank on the side of the cryostat. Operating on the telescope, the helium-3 hold time is 60 h, the helium-4 hold time is 48 h, and the liquid nitrogen lasts for 40 h. In normal operation, the nitrogen vessel is topped up once per day, and the helium-3 system is re-cycled on alternate days.

The helium-3 refrigerator employs an exchange-gas pump to control the temperature of the main helium-3 pump. It thus avoids the use of any mechanical heat switches. More details of the refrigerator are given in Griffin (1985).

The optical components within the cryostat are installed in such a way that the receiver can easily be assembled and disassembled (e.g. for the installation of test filters).

6 RECEIVER OPERATION ON THE JCMT

6.1 Data collection

The signal from the detector pre-amplifier is fed to a phase-sensitive detector (PSD) which is also located on the Nasmyth platform. The output from the PSD is fed to a voltage to frequency converter, the output of which goes directly to the VAX computer. An on-line de-spiking routine is applied to the individual data samples, and values which differ from the mean by more than a preset number of standard deviations (usually 5) are rejected. The individual pairs, together with their associated statistical errors, are stored on disc. A real-time display of the signal and signal-to-noise is presented on a terminal during the course of the integration.

6.2 Set-up selection

The filter, iris and PSD (gain, phase, time constant) can all be set by the observer from the control terminal. A continuous analogue monitor is provided for both the in-phase and out-of-phase channels on a chart recorder.

6.3 Sky chopping

Sky chopping is necessary to remove most of the telescope and atmospheric contributions to the signal. The JCMT secondary mirror (van der Stadt 1987) can be nutated to provide a chop throw of up to 8 arcmin at 3 Hz and up to 2 arcmin at 8 Hz with 80 per cent duty cycles. The chop frequency is usually set at 7.8 Hz with chop throws up to 2 arcmin. If a larger throw is required, the chopping frequency must be reduced. Very large chop throws are performed at the expense of additional sky noise due to the reduction in the achievable temporal and spatial atmospheric correlation imposed by large slow chops. Although the secondary can be nutated about any axis, allowing one to chop in any direction, most observations are made with an azimuthal chop. Three-beam chopping is also available for use in high sky noise conditions (see Section 7.3).

6.4 Five-point routine

The JCMT pointing accuracy is currently about 1–2 arcsec rms. It is usually necessary to refine the pointing using a sufficiently bright point-like source in the vicinity of the target object. A catalogue of pointing sources (brighter than about 1 Jy at 1.1 mm) is available for this purpose. An automatic five-point routine may be used which performs a two-dimensional Gaussian fit to the five points and derives the local telescope offsets in azimuth and elevation.

6.5 Mapping

Continuum mapping with UKT14 can currently be carried out by making a raster using either single step-and-integrate or by continuous scanning, the latter technique being referred to as 'on-the-fly' mapping. The former can be performed in two different modes: (i) beamswitch mode in which the telescope and secondary are both nodding and chopping during the map, and (ii) differential mapping in which the telescope nodding is suppressed while chopping continues.

In the beamswitch mode the chop throw is made large enough to ensure that there is no emission in the reference beam and at each point in the map both the signal and reference beam are observed and the difference between them is recorded. Typical chop throws in this mode range from 90 to 200 arcsec. Mapping in beamswitch mode is possible in any standard coordinate system, as well as in user-defined coordinate frames. In the differential mapping mode the telescope nodding is inhibited and each grid point is only observed in the signal beam. The chop throw is much smaller and typically 60 arcsec but the map is made large enough so that the signal and the reference beam will be completely off source at the edges of the map. In this mode the mapping may currently be carried out only in altitude-azimuth because the scanning has to be performed in the chop direction, and the secondary cannot yet be controlled to follow a rotating coordinate frame. The resulting map is then deconvolved using the NOD2 software (Haslam 1974) and converted to equatorial coordinates.

The obvious drawback of the first technique is the uncertainty as to whether the chop throw is sufficient to position the reference beam completely off-source, whereas with the differential technique the resulting map can be immediately examined to test whether the map has been made large enough. However, a drawback of differential mapping is that a larger area must be mapped than for the beamswitched case because, due to the deconvolution, half the chop throw is lost at the edges of the map. Since sky noise is often the dominating noise source in the map, the beamswitch mode tends to gain during severe sky conditions, because of better sky cancellation. Using the differential mode in severe sky noise the chop throw can be further reduced. Although the deconvolution of the differential dual beam maps is known to cause additional noise if the map is larger than 2.5 times the chop throw (Emerson, Klein & Haslam 1979), experi-

Table 3. Measured beamwidths for a surface accuracy of 40 μm RMS.

FILTER	APERTURE (mm)	FWHM BEAMWIDTH (ARCSEC)
2.0 mm	65	27.2
1.3 mm	65	19.5
1.1 mm	65	18.5
800μm	65	16.0
	47	13.5
600μm	65	17.2
450μm	65	17.5
	27	10.0
350μm	65	19.0

ence has shown that in the submillimetre regime there is a general gain by using a small chop throw because of the substantial reduction in sky noise.

7 RECEIVER PERFORMANCE

7.1 Beam widths

The half-power beamwidths (HPBW) which have been measured to date are summarized in Table 3. It should be noted that the beam shape and width are subject to change as the panels making up the telescope primary are adjusted to improve the surface accuracy of the antenna. The greatest change in gain and beam shape will be at the shortest wavelengths. The HPBW presented correspond to an rms surface error somewhat under 40 μm. The beam shape at short wavelengths will also have additional chop amplitude dependence (due to coma caused by the tilting of the secondary when chopping).

7.2 Receiver sensitivity

The overall sensitivity is represented by the noise equivalent flux density (NEFD). This is the flux density (outside the earth's atmosphere) which produces a signal-to-noise of one in one second of integration. Values under typical observing conditions are 350 mJy at 1100 μm, 500 mJy at 800 μm and 4 Jy at 450 μm. Note how the shorter wavelength sensitivity is far more sensitive to the atmospheric conditions. It is often the case that observations at wavelengths below 800 μm are not possible due to low transmission, high excess sky noise or both. Under the best conditions, the sensitivity at 350 μm is limited by photon noise from the sky and the telescope, and the 1.1 mm sensitivity is limited partly by the background but mainly by the detector noise. The point-source sensitivity at 1.1 mm is more than a factor of 10 better than on UKIRT, due to the larger collecting area.

7.3 Sky noise and 3-position chopping

Temporal and spatial variations of the atmospheric emission often lead to higher NEFDs. Unfortunately, these increases are not limited to times of poor transmission, and the submillimetre wavelengths can suffer from considerable excess noise of a '$1/f$' type spectrum even in conditions of excellent transmission (Duncan & Robson 1989, in preparation).

Temporal variations are minimized by chopping faster than the typical correlation time of the atmospheric fluctuations. Spatial variations exist because the two beams given by chopping are looking through different atmospheric paths and the atmosphere has gradients in emission. Thus the two beams of conventional chopping do not completely cancel the spatial variations and excess noise is present in the chopped signal. This noise is extremely difficult to integrate out because it has significant low-frequency content and is non-stationary. A typical integration, in the presence of sky noise, will go down to a certain level and then the standard error of the integrated noise will flatten out.

The gradient in emission is primarily linear for chop throws of a few arcmin, therefore a chop waveform which rapidly places 3 beams on the sky can take out the linear variations in emission and greatly reduce the effect of '$1/f$' fluctuations on the measured noise. A fuller explanation of this method of sky noise reduction is given by Papoular (1983). This mode of chopping is available at JCMT for use in high sky noise situations and the preferred mode of chopping under various sky noise conditions is under continuing investigation.

8 FUTURE DEVELOPMENTS

8.1 Focal plane calibration system

Submillimetre continuum observations have typically been calibrated by monitoring the signal from a bright source at various airmasses to determine the atmospheric extinction. This method is subject to major errors due to the lack of homogeneity of the atmosphere. The water vapour content of the atmosphere is a function of time and position of the object in the sky. Hence, the poor sky coverage available from bright calibration sources can often make it extremely difficult to determine accurately the atmospheric transmission at the position of the source. To overcome this problem, a focal plane calibration system is under construction which will allow the periodic monitoring of the sky emission wherever the antenna is pointing. This will be done by comparing the sky with an ambient load and a liquid nitrogen cooled load using a focal plane chopper wheel, and by doing sky dips (measuring the sky temperature versus airmass) in order to determine the local extinction. This calibration system will be available during 1990.

8.2 Polarimeter

A submillimetre polarimeter is under development by the University of Aberdeen in collaboration with Queen Mary College. It will operate at 1.1, 0.8 and 0.45 mm, and will be mounted directly in front of UKT14 on the Nasmyth platform. The polarimeter will be tested on the telescope in autumn 1989.

8.3 Bolometer array

The next generation submillimetre receiver for the JCMT is already in the design phase. This instrument, called SCUBA (Submillimetre Common User Bolsometer Array), will be an imaging receiver with two diffraction-limited arrays operating simultaneously at 450 and 850 μm. Imaging will also be possible at 750, 600 and 350 μm, and single-channel photo-

metry will be possible in all of the atmospheric windows up to 1100 μm. The detectors will be cooled to around 100 mK to achieve sky photon noise-limited sensitivity, offering a dramatic improvement in sensitivity over any submillimetre photometer currently in existence. SCUBA is being constructed by the Royal Observatory Edinburgh in collaboration with Queen Mary College, and is expected to be in user operation in 1992.

ACKNOWLEDGMENTS

We, and in particular WDD, wish to thank the staff of the Technology Unit and Workshop of the Royal Observatory Edinburgh for their help and assistance.

REFERENCES

Ade, P. A. R., Griffin, M. J., Cunningham, C. T., Radostitz, J. V., Predko, S. & Nolt, I. G., 1984. *Infrared Phys.*, **24,** 403.
Altenhoff, W. J., Baars, J. W. M., Downes, D. & Wink, J. E., 1987. *Astr. Astrophys.*, **184,** 381.
Duncan, W. D., 1983. *Infrared Phys.*, **23,** 333.
Edelson, R. A., Gear, W. K., Malkan, M. A. & Robson, E. I., 1988. *Nature,* **336,** 749.
El-Ataway, S., Ade, P. A. R., Radostitz, J. V. & Nolt, I. G., 1980. *Int. J. Infrared Millimeter Waves,* **1,** 459.
Emerson, D. T., Klein, V. & Haslam, C. G. T., 1979. *Astr. Astrophys.*, **76,** 92.
Emerson, J. P., 1988. *Formation and Evolution of Low Mass Stars,* Proc. of the Nato Advanced Study Institute, p. 193, eds Dupree, A. K. & Lago, M. T. V. T., Kluwer, Dordrecht.
Griffin, M. J., 1985. *PhD thesis,* University of London.
Griffin, M. J. & Holland, W. A., 1988. *Int. J. Infrared Millimeter Waves,* **9,** 861.
Harper, D. A., Hildebrand, R. H., Steining, R. & Winston, R., 1976. *Appl. Opt.*, **15,** 53.
Haslam, C. G. T., 1974. *Astr. Astrophys. Suppl.*, **15,** 333.
Kemp, A. J., 1980. *Int. J. Infrared Millimeter Waves,* **1,** 469.
Papoular, R., 1983. *Astr. Astrophys.*, **117,** 46.
van der Stadt, H., 1987. *Appl. Opt.*, **26,** 3446.
Watt, G. D. & Webster, A. S. (eds), 1990. *Submillimetre Astronomy,* Kluwer, Dordrecht.
Wolstencroft, R. D. & Burton, W. B. (eds), 1988. *Millimetre and Submillimetre Astronomy,* Kluwer, Dordrecht.